ACS APPLIED MATERIALS & INTERFACES

Research Article

www.acsami.org

Aqueous Synthesis of Silver Nanoparticle Embedded Cationic Polymer Nanofibers and Their Antibacterial Activity

Jooyoung Song, Haeyoung Kang, Choonghyeon Lee, Sun Hye Hwang, and Jyongsik Jang*

WCU program of Chemical Convergence for Energy and Environment (C2E2), School of Chemical and Biological Engineering, College of Engineering, Seoul National University, 599 Gwanak-ro, Gwanak-gu, Seoul 151-742, Korea

Supporting Information

ABSTRACT: This paper describes the one-pot, aqueous synthesis of cationic polymer nanofibers with embedded silver nanoparticles. Poly[2-(*tert*-butylaminoethyl) methacrylate] (PTBAM) was used as a cationic polymer substrate to reinforce the antimicrobial activity of the embedded silver nanoparticles. Electron microscope analyses revealed that the as-synthesized nanofibers had diameters of approximately 40 nm and lengths up to about 10 μm. Additionally, silver nanoparticles of approximately 8 nm in diameter were finely embedded into the prepared nanofibers. The embedded silver nanoparticles had a lower tendency to agglomerate than colloidal silver nanoparticles of comparable size. In addition, the nanofibers with embedded silver nanoparticles exhibited excellent antibacterial performance against Gram-negative *Escherichia coli* and Gram-positive *Staphylococcus aureus*. Interestingly, the prepared nanofibers exhibited enhanced bactericidal performance compared with the silver-embedded poly(methyl methacrylate) (PMMA) nanofibers, presumably because of the antibacterial properties of the PTBAM substrate.

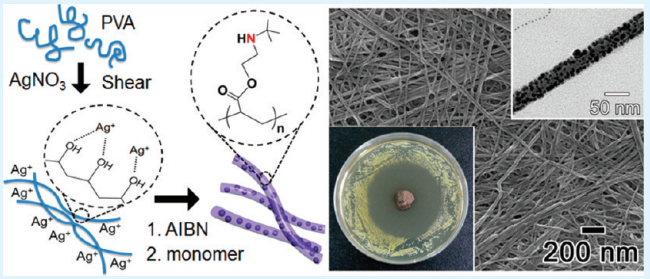

KEYWORDS: *silver, nanoparticles, cationic polymer, nanofiber, antibacterial, nanocomposite*

INTRODUCTION

With increasing concerns of microbial infections, there is growing interest in the development of new, effective antimicrobial agents.[1−6] Silver is an excellent antimicrobial agent because of its broad-spectrum biocidal activity and limitation of development of resistant microbial strains.[7−9] In an in-depth study, Morones et al. demonstrated the bactericidal effect of silver nanoparticles with sizes in the range of 1−100 nm.[7] Alt et al. reported the in vitro antibacterial activity of nanosilver against multiresistant bacteria and the in vitro cytotoxicity of silver nanoparticles loaded into poly(methyl methacrylate) (PMMA) bone cement.[10] Although not fatal, silver nanoparticles have shown toxicity toward mammalian cells.[11−14] The toxicity of colloidal silver nanoparticles has been attributed to uptake of silver nanoparticles by cells or to the oxidative release of silver cations from the surface of the silver nanoparticles that can affect basic functions in mammalian cells.[13] From this viewpoint, immobilization of nanosilver onto adequate substrates is advantageous because it inhibits direct uptake of the nanoparticles by cells. In addition, compared to colloidal silver nanoparticles, immobilized silver nanoparticles effectively resist oxidation and aggregation, which can reduce the antibacterial efficiency.[15,16] There are numerous reports on the silver nanocomposites and their antibacterial performances.[15−23] For example, Lu et al. reported that silver nanoparticles embedded into silicon nanowires are much more stable and resistant to aggregation than colloidal silver nanoparticles.[16]

The antibacterial performance is time-limited in silver-containing materials that kill bacteria via the release of silver ions or silver nanoparticles.[20,21] To improve the durability of biocidal activity, researchers have suggested incorporation of silver into biocidal polymers.[21−23] Quaternary ammonium compounds,[25−27] antimicrobial peptides,[28,29] and rhodanine derivatives[22−24] are strong candidates for use as antibacterial substrates because of their contact-active bactericidal properties. Therefore, composites of these materials with silver nanoparticles are promising for long-term and efficient antimicrobial performance. For example, Rubner et al. reported a dual-functional bactericidal coating based on a two-level coating of quaternary ammonium silane and silver.[21] These composites maintained antibacterial performance even after the contained silver was depleted. To date, this kind of research has been limited to the incorporation of silver into bulk substrates.

This paper reports the one-step fabrication of silver nanoparticles embedded into poly[2-(*tert*-butylaminoethyl) methacrylate] (Ag/PTBAM) nanofibers by radical-mediated dispersion polymerization. We evaluated the antimicrobial performance of these Ag/PTBAM composites. It has been reported that poly[2-(*tert*-butylaminoethyl) methacrylate] (PTBAM) has high antibacterial activity and low toxicity to human cells.[30,31] The pendant bulky secondary amine of

Received: November 9, 2011
Accepted: December 19, 2011
Published: December 19, 2011

Scheme 1. Illustration of the Synthetic Procedure of Silver Nanoparticles Embedded PTBAM Nanofibers

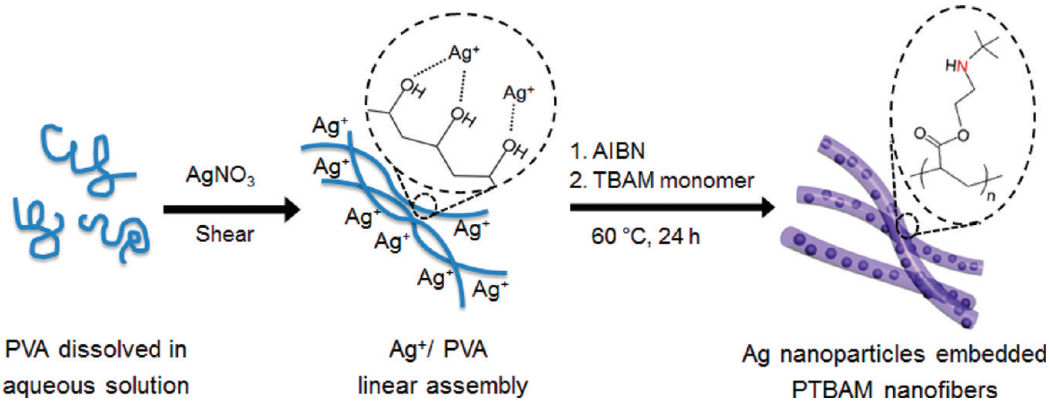

PTBAM causes phase separation of lipid layers inside bacteria, resulting in cell death. Moreover, in contrast to other amine-containing polycationic substances, PTBAM exhibits bactericidal activity without additional quaternization.[32−34] The nanosize fibrous morphology of PTBAM leads to Ag/PTBAM composites with very high surface area, which in turn leads to higher cell attachment and higher silver release.[22,35,36] Our results revealed that the synthesized silver nanoparticles embedded into PTBAM nanofibers had enhanced antibacterial efficacy compared to silver sulfadiazine (SSD), silver nitrate, and silver nanoparticles embedded into PMMA nanofibers against Gram-negative *Escherichia coli* (*E. coli*) and Gram-positive *Staphylococcus aureus* (*S. aureus*).

EXPERIMENTAL SECTION

Materials. The monomers 2-(*tert*-butylamino)ethylmethacrylate (TBAM) and methylmethacrylate were purchased from Aldrich (St. Louis, MO). TBAM was used without further purification, and methylmethacrylate was used after purification with an inhibitor remover. Poly(vinylalcohol) (PVA) (M_w: 124 000−186 000), silver nitrate ($AgNO_3$), and silver sulfadiazine (SSD) were also obtained from Aldrich (St. Louis, MO). The initiator 2,2-azobis-(isobutyronitrile) (AIBN) was obtained from Junsei Chemical Co., Ltd. (Japan). All purifications and reactions were carried out under atmospheric pressure.

Fabrication of Silver Nanoparticles Embedded into Polycationic Nanofibers. PVA was dissolved in deionized water (1.0 g to 200 mL). Silver precursor, $AgNO_3$ (0.118 mmol), was added to the PVA solution and stirred for 1 h with a magnetic stirring bar. Next, 0.75 mL of a methylene chloride solution containing AIBN (0.6 mmol) was injected into the PVA solution, followed by the addition of 0.4 mL of TBAM monomer. The polymerization of TBAM and the reduction of silver ions proceeded under vigorous stirring at 60 °C for 24 h. After polymerization, the synthesized Ag/PTBAM nanofibers were centrifuged and washed with an excess amount of methanol to remove residual reagents.

Instrumentation. Energy-filtering transmission electron microscopy (EF-TEM) images were obtained with a Carl Zeiss LIBRA 120 at an acceleration voltage of 120 kV. In the sample preparation, Ag/PTBAM nanofibers were cast onto a copper grid after dilution in aqueous solution. Field-emission scanning electron microscopy (FE-SEM) images were obtained using a JEOL 6700 at an acceleration voltage of 10 kV. Fourier transform infrared (FT-IR) spectra were recorded on a Bomem MB100 spectrometer (Quebec, Canada) in transmittance mode at a resolution of 4 cm^{-1} and 32 scans. Ultraviolet−visible (UV−vis) spectra were obtained at 25 °C with a PerkinElmer Lambda-20 spectrometer. X-ray photoelectron spectroscopy (XPS) was performed with a SIGMA PROBE (ThermoVG, U.K.).

Antimicrobial Tests. For the modified Kirby-Bauer test, solid-state SSD and Ag/PTBAM nanofibers were pressed into a disk shape with a diameter of 13 mm using a hydraulic press. The prepared samples had equal amount of silver. Separately, 50 μL of *S. aureus* suspension (10^6−10^7 CFU/mL) was cultured on Luria−Bertani (LB) agar plates. Then, each prepared sample disk was gently placed on the center of the bacteria growth on the LB agar plates and incubated overnight at 37 °C. Bacterial colony growth was observed, and the zone of inhibition was measured to evaluate the antibacterial performance.

For the kinetic test, *E. coli* and *S. aureus* were prepared. The culture medium of each bacterium was inoculated with bacteria and incubated overnight at 37 °C. Bacterial growth rates were measured by monitoring the optical density at 600 nm (OD_{600}) using a spectrophotometer. The incubated bacteria were injected to fresh media and grown at 37 °C with 200 rpm of shaking to an OD_{600} of 0.1. Various concentrations of Ag/PTBAM nanofibers and SSD (from 1 to 25 μg/mL) were then added to the culture, and the OD_{600} was measured over time.

A minimum inhibition concentration (MIC) test was performed as follows. The Ag/PTBAM nanofibers were dispersed in aqueous solution for the MIC test. Nanofibers of PMMA with embedded silver nanoparticles (Ag/PMMA) were fabricated according to a reported procedure and used as a control.[37] An aqueous solution of $AgNO_3$ was also prepared and used for comparative tests. To obtain the concentration of silver in these prepared solutions, the samples were dissolved in aqua regia. After 24 h, the solutions were diluted 100-fold, and the concentrations of Ag were measured by inductively coupled plasma atomic emission spectrometry (ICP-AES). For the test, 5 mL of sterilized LB agar solutions were inoculated with each bacterium (1×10^5 to 1×10^6 CFU). Then, the prepared samples were added to the bacteria suspensions at different concentrations and incubated at 37 °C while shaking at 200 rpm. After 24 h, fresh organisms were reinoculated and incubated for an additional 24 h. Growth or no-growth was determined by visual inspection. For accuracy of the results, all of the concentration values were analyzed three times and averaged. The standard deviation was less than 5%.

RESULTS AND DISCUSSION

The synthesis of Ag/PTBAM nanofibers by radical-mediated dispersion polymerization is illustrated in Scheme 1. Silver ions (Ag^+) were added to an aqueous solution of PVA and were coordinated to hydroxyl groups on the PVA. The Ag^+−PVA complex was linearly assembled due to high shear under vigorous stirring. AIBN was then added to the Ag^+−PVA aqueous solution at 60 °C. AIBN acted as a reducing agent for the silver ions and as a radical initiator for the TBAM monomer. The silver nanoparticle−PVA complexes (Ag−PVA) were linearly and tightly assembled due to both the high shear conditions and dipole−dipole interactions between silver

dx.doi.org/10.1021/am201563t | ACS Appl. Mater. Interfaces 2012, 4, 460−465

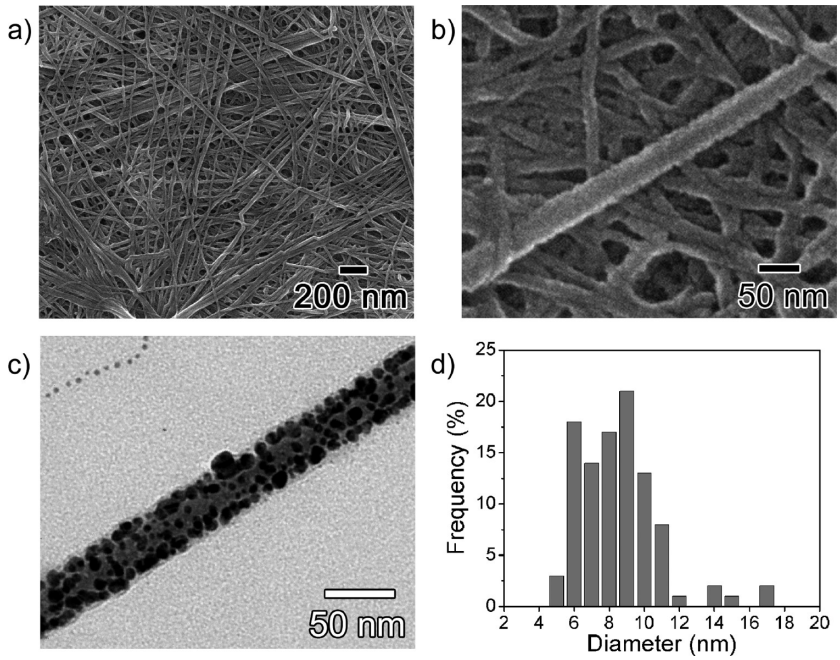

Figure 1. (a, b) FE-SEM and (c) TEM images of the silver nanoparticles embedded PTBAM nanofiber and (d) size distribution of the embedded silver nanoparticles. The silver nanoparticle size was determined via randomly counting 100 Ag nanoparticles by TEM.

nanoparticles.[38] When TBAM monomer was injected into the reaction medium, the carboxyl groups of the TBAM monomer formed hydrogen bonds with the hydroxyl groups of PVA.[37] PVA acted as a gelator to form and grow nanofibers in the axial direction and also acted stabilizer to disperse silver nanoparticles.[37] The TBAM monomer was polymerized onto the Ag−PVA complex for 24 h via radical polymerization using AIBN as an initiator, after which Ag/PTBAM nanofibers were obtained. When the experiments proceeded without $AgNO_3$, the products had atypical morphology with micrometer size rather than fibrous nanostructure (see Figure S1 in the Supporting Information). Although the mechanism is still not clear, it can be considered that the silver nanoparticles play an important role in formation of fibrous nanostructure.

EF-TEM and FE-SEM images in Figure 1 show the morphology of the fabricated Ag/PTBAM composite nanofibers. As shown in the FE-SEM image (Figure 1a, b), the synthesized composite nanofibers had fibrous morphology; the average diameter and length of the polymer nanofibers were approximately 40 nm and greater than 10 μm, respectively. It was confirmed using EF-TEM that silver nanoparticles of average 8.5 nm in diameter were finely embedded throughout the polymer nanofibers (Figure 1c, d). Additionally, the synthesized Ag/PTBAM nanofibers possessed a smooth surface morphology (Figure 1b), which indicates that the silver nanoparticles were not located on the surface but were instead embedded inside the PTBAM polymer nanofiber. Importantly, we verified what we found in our previous studies, namely that a nanofibrous structure could be obtained using radical-mediated dispersion polymerization.[37]

The optical properties of the Ag/polymer nanofibers were analyzed by absorption spectroscopy. To verify polymerization of the PTBAM, we performed FTIR analysis. A peak near 3400 cm^{-1} was observed in the FTIR spectrum of the Ag/PVA−PTBAM and was attributed to the O−H stretching vibration of PVA.[37] Peaks at 1738 cm^{-1} and in the 1550−1610 cm^{-1} region were attributed to C═O stretching and COO asymmetric vibrations of PTBAM.[39] In addition, peaks at 1230 and 1150 cm^{-1} were attributed to C−N stretching modes.[39] The peak at 2200 cm^{-1} originated from C≡N bonding in AIBN, which was used as a reducing agent and an initiator. In the UV−vis spectra (Figure 2b), the plasmon absorption peak at 402 nm was characteristic of nanosized silver particles; the broadness of this peak was indicative of the polydisperse and nanoscale size of these nanoparticles.[40,41] An XPS spectrum of the Ag/PTBAM composite is presented in Figure 2c; the two peaks at 369 and 375 eV, with 6.0 eV separation, corresponded to the Ag $3d_{5/2}$ and Ag $3d_{3/2}$ binding energies, respectively.[42] We concluded from the spectral data that the Ag/PTBAM nanofiber composite had negligible shifts from and the same spin energy separation as metallic silver, implying that the synthesized silver nanoparticles were mostly zerovalent. Based on these data, the polymerization was successfully carried out on the surface of the silver−PVA complex, which led to the formation of PTBAM nanofibers with embedded silver nanoparticles. In addition, thermogravimetric analysis (TGA) confirmed that the synthesized Ag/PTBAM nanofibers contained about 55 wt % silver (see Figure S2 in the Supporting Information). In addition, as shown in Figure S3, the silver nanoparticles in the Ag/PTBAM nanofibers had a lower tendency toward aggregation than colloidal silver nanoparticles without stabilizer.[16,43,44] It can be considered that the polymer substrate prevented aggregation of the embedded silver nanoparticles.

The antibacterial performance of prepared Ag/PTBAM nanofibers was investigated using a modified Kirby-Bauer technique. SSD, a known anti-inflammatory ingredient, was chosen as a comparative material. Ag/PTBAM nanofibers and SSD were made into discs with diameters of approximately 13 mm and placed on a bed of *S. aureus* in an agar plate. The antibacterial properties were measured by evaluating the zone of inhibition around the disk after incubation at 37 °C (Figure 3). The diameter of the zone of inhibition for the Ag/PTBAM nanofiber composite disk was approximately 50.2 mm, whereas that of the SSD disk was approximately 17.6 mm. These results

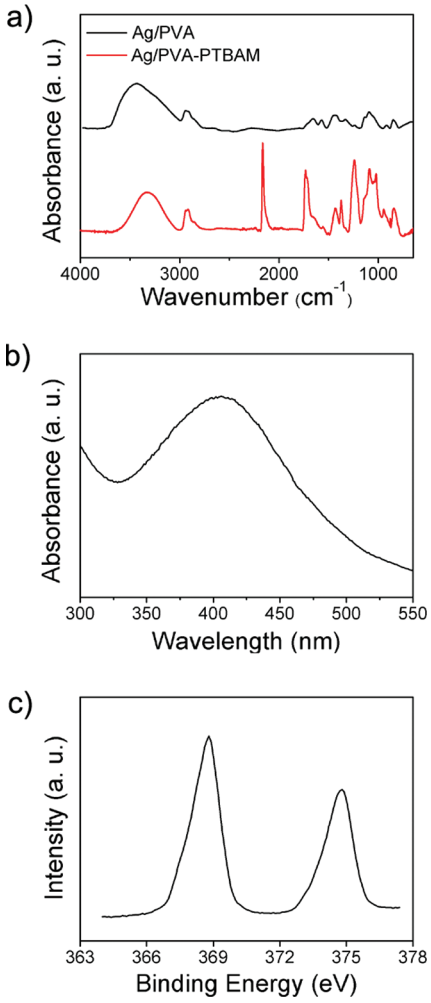

Figure 2. (a) FT-IR spectra of Ag-PVA composite and the fabricated silver embedded polymer nanofibers and (b) UV–vis spectrum and (c) XPS spectrum of the Ag nanoparticles embedded poly(TBAM) nanofibers.

indicated that the Ag/PTBAM nanofibers exhibited superior performance as an antibacterial agent compared to SSD. The SSD slowly releases silver ions as an antibacterial agent,[20] and it is possible that the diffusion of silver ions was blocked by the formation of secondary compounds such as silver chloride in the Kirby-Bauer test media.[42] However, in the case of Ag/PTBAM nanofibers, the PTBAM substrate is sufficiently porous to allow water to pass through the nanofibers.[45] Thus, silver nanoparticles (or silver ions) embedded in the PTBAM nanofibers could easily diffuse into the test media and act as biocidal agents.

A bacterial inhibition growth curve was used to study the growth kinetics of *E. coli* and *S. aureus* with prepared biocidal samples (Figure 4). The optical density at 600 nm (OD_{600}) was measured to monitor bacterial growth; the bacteria were grown to an OD_{600} of 0.1 and then various concentrations of Ag/PTBAM nanofibers or SSD were added to the bacterial solution.[46] In both cases, the bacterial growth was delayed as the concentration of silver compounds increased, but the rates of bacterial growth delay were different. The growth of *E. coli* was completely inhibited by the Ag/PTBAM nanofibers when the concentration of nanofibers is 10 μg/mL. The SSD inhibited growth of *E. coli* at 25 μg/mL. In addition, Ag/PTBAM nanofibers with 5 μg/mL of concentration were able to slow the growth of *S. aureus,* whereas SSD slowed its growth at 10 μg/mL. These results confirmed that the Ag/PTBAM nanofibers possessed enhanced antimicrobial activity compared to SSD. Both silver ions and silver nanoparticles exhibit antibacterial properties via similar mechanisms, such as interactions with bacterial membranes or binding with metabolic materials.[7,15] However, for the same total silver concentration, the silver nanoparticles in Ag/PTBAM exhibited significantly higher antibacterial effects than the silver ions in SSD. When silver ions come into contact with bacteria, precipitates are formed, and the antimicrobial ability of SSD deteriorates.[47] In contrast, the Ag/PTBAM nanofibers release silver nanoparticles, which come into contact with bacteria without direct precipitation. Therefore, the prepared Ag/PTBAM nanofibers, which contained silver nanoparticles, showed higher bactericidal efficacy than SSD, which contained only silver ions. The nanometer-sized PTBAM polymer nanofibers also provided a large surface area for more effective antimicrobial performance.[35,36]

Finally, we evaluated the extent to which the antibacterial properties of the PTBAM substrate itself contributed to its excellent antibacterial activities. An MIC test was performed to verify the biocidal properties of PTBAM nanofibers. Nanofibers with diameters similar to PMMA (which has no specific

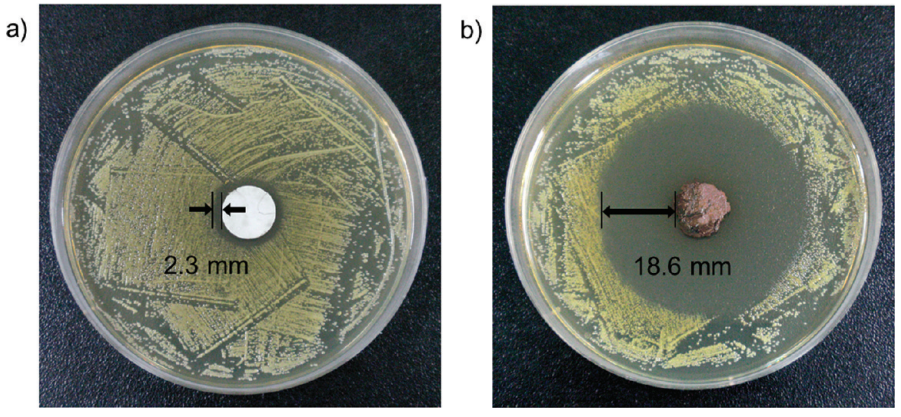

Figure 3. Photograph images of the zone of inhibition of (a) silver sulfadiazine and (b) silver/PTBAM nanofiber by the modified Kirby-Bauer test. Two silver compounds were pressed by hydraulic press to obtain disk shape and placed on the lawn of *S. aureus.* After 12 h of incubation, the zone of inhibition was measured. Both disk sizes are ca. 13 mm in diameter.

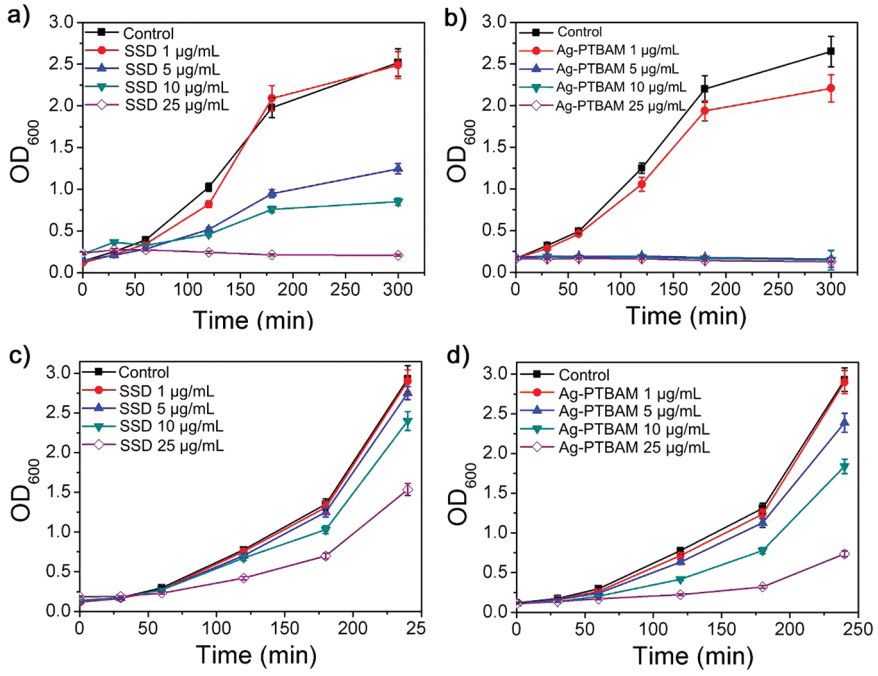

Figure 4. Bacterial growth curve in LB media. Different concentrations of silver sulfadiazine (SSD) or silver nanoparticles embedded cationic polymer nanofiber (Ag/PTBAM) were added to the (a, b) *E. coli* and (c, d) *S. aureus* culture. The growth of the bacteria was monitored measuring the optical density at 600 nm.

Table 1. Minimum Inhibitory Concentration Tests of Various Silver Compounds[a]

	Ag/PTBAM			Ag/PMMA			$AgNO_3$	
bacteria	concn of Ag (ng/mL)[b]	24 h	48 h	concn of Ag (ng/mL)[b]	24 h	48 h	concn of Ag (ng/mL)[b]	24 h	48 h
E. coli	1718	−	−	1667	−	−	1783	−	−
	859	−	−	834	−	−	892	−	+
	430	−	−	417	−	−	446	−	+
	215	−	−	208	−	−	223	+	+
	107	−	−	104	−	−	111	+	+
	53.7	−	−	52.1	−	+	55.7	+	+
	26.8	−	+	26.1	+	+	27.9	+	+
	13.4	+	+	13.0	+	+	13.9	+	+
S. aureus	17182	−	−	16673	−	−	17831	−	+
	8591	−	−	8337	−	−	8915	+	+
	4296	−	−	4168	−	−	4458	+	+
	2148	−	−	2084	−	+	2229	+	+
	1611	−	+	1563	−	+	1670	+	+
	1074	+	+	1042	+	+	1114	+	+

[a]LB liquid media was clear before incubation with 2×10^4 to 1×10^5 per mL of *E.coli* or *S.aureus*; "−" no growth; "+"growth. [b]The concentration of Ag in the silver compounds was measured by ICP-atomic emission spectrometer with aqua-regia treatment.

biocidal activity) were prepared for comparison with silver nanoparticle-embedded PMMA (see Figure S4 in the Supporting Information). The MIC value of $AgNO_3$ was also obtained for comparison. Serial concentrated solutions were each incubated with equal volumes of *E. coli* and *S. aureus* suspensions. The concentrations of the sample solutions were adjusted based on silver content. Growth or no-growth of bacteria was determined by visual inspection. In the case of Gram-negative *E. coli*, the MIC of Ag/PTBAM nanofibers was about two times lower that of Ag/PMMA nanofibers and about 16 times lower than that of $AgNO_3$ after 24 h incubation (Table 1). An additional 24 h after inoculation with fresh bacteria, the MIC values at 48 h were higher than those at 24 h because of the addition of new organisms. An MIC test against Gram-positive *S. aureus* was also performed. In this case, the Ag/PTBAM nanofibers exhibited enhanced antibacterial activity compared to both Ag/PMMA nanofibers and $AgNO_3$. Notably, the Ag/PTBAM nanofibers had higher bactericidal efficiencies than Ag/PMMA nanofibers, which was attributed to the additional antibacterial performance of the PTBAM substrate. The pendant amino groups of PTBAM act as bactericides by inducing phase separation of charged and uncharged lipids inside the cytoplasma membrane of bacteria.[30,48] Eventually, the cytoplasma membrane disintegrates, which causes death of the microorganism.[30,48] For this reason, it was anticipated that Ag/PTBAM nanofibers would exhibit bactericidal activity to some degree even after depletion of the embedded silver nanoparticles. On the basis of these

dx.doi.org/10.1021/am201563t | *ACS Appl. Mater. Interfaces* 2012, 4, 460−465

data, our synthesized Ag/PTBAM nanofibers had enhanced antibacterial performance because of the antibacterial properties of both the PTBAM nanofibers alone and the embedded silver nanoparticles.

In conclusion, PTBAM nanofibers with embedded silver nanoparticles were synthesized using one-pot, radical-mediated dispersion polymerization under aqueous conditions. The embedded silver nanoparticles exhibited a lower tendency toward aggregation compared with colloidal silver nanoparticles. The fabricated Ag/PTBAM nanofibers had enhanced antibacterial activities against both Gram-negative *E. coli* and Gram-positive *S. aureus* based on the bactericidal properties of both the silver nanoparticles and the PTBAM substrate. These results suggest that Ag/PTBAM nanofibers have potential for use in biofilms and hygienic and antiadhesion applications.

■ ASSOCIATED CONTENT

Ⓢ Supporting Information

FE-SEM image of PTBAM without silver nanoparticles (Figure S1), TGA data of Ag/PTBAM nanofiber (Figure S2), UV−vis spectroscopy of the silver compounds (Figure S3) and FE-SEM and TEM images of Ag/PMMA nanofiber (Figure S4). This information is available free of charge via the Internet at http://pubs.acs.org/.

■ AUTHOR INFORMATION

Corresponding Author

*E-mail: jsjang@plaza.snu.ac.kr. Telephone: (+82) 2-880-7069. Fax: (+82) 2-888-1604.

■ ACKNOWLEDGMENTS

This research was supported by WCU (World Class University) program through the National Research Foundation of Korea funded by the Ministry of Education, Science and Technology (R31-10013).

■ REFERENCES

(1) Chen, C.; Pan, F.; Zhang, S.; Hu, J.; Cao, M.; Wang, J.; Xu, H.; Zhao, X.; Lu, J. R. *Biomacromolecules* **2010**, *11*, 402−411.
(2) Neoh, K. G.; Kang, E. T. *ACS Appl. Mater. Interfaces* **2011**, *3*, 2808−2819.
(3) Dong, A.; Lan, S.; Huang, J.; Wang, T.; Zhao, T.; Xiao, L.; Wang, W.; Zheng, X.; Liu, F.; Gao, G.; Chen, Y. *ACS Appl. Mater. Interfaces* **2011**, *3*, 4228−4235, DOI: 10.1021/am200864p.
(4) Han, H.; Wu, J.; Avery, C. W.; Mizutani, M.; Jiang, X.; Kamigaito, M.; Chen, Z.; Xi, C.; Kuroda, K. *Langmuir* **2011**, *27*, 4010−4019.
(5) Bujdák, J.; Jurečeková, J.; Bujdáková, H.; Lang, K.; Šeršeň, F. *Environ. Sci. Technol.* **2009**, *43*, 6202−6207.
(6) Kong, H.; Song, J.; Jang, J. *Environ. Sci. Technol.* **2010**, *44*, 5672−5676.
(7) Morones, J. R.; Elechiguerra, J. L.; Camacho, A.; Holt, K.; Kouri, J. B.; Ramírez, J. T. *Nanotechnology* **2005**, *16*, 2346−2353.
(8) Kumar, A.; Vemula, P. K.; Ajayan, P. M.; John, G. *Nat. Mater.* **2008**, *7*, 236−241.
(9) Van Waasbergen, L. G.; Fajdetic, I.; Fianchini, M.; Rasika Dias, H. V. *J. Inorg. Biochem.* **2007**, *101*, 1180−1183.
(10) Alt, V.; Bechert, T.; Steinrücke, P.; Wagener, M.; Seidel, P.; Dingeldein, E.; Domann, E.; Schnettler, R. *Biomaterials* **2004**, *25*, 4383−4391.
(11) Yen, H.-J.; Hsu, S.-H.; Tsai, C.-L. *Small* **2009**, *5*, 1553−1561.
(12) Asharani, P. V.; Mun, G. L. K.; Hande, M. P.; Valiyaveettil, S. *ACS Nano* **2009**, *3*, 279−290.
(13) Grunlan, J. C.; Choi, J. K. *Biomacromolecules* **2005**, *6*, 1149−1153.
(14) Panacek, A.; Kolar, M.; Vecerova, R.; Prucek, R.; Soukupova, J.; Krystof, V.; Hamal, P.; Zboril, R.; Kvitek, L. *Biomaterials* **2009**, *30*, 6333−6340.
(15) Dallas, P.; Sharma, V. K.; Zboril, R. *Adv. Colloid Interface Sci.* **2011**, *166*, 119−135.
(16) Lv, M.; Su, S.; He, Y.; Huang, Q.; Hu, W.; Li, D.; Fan, C.; Lee, S.-T. *Adv. Mater.* **2010**, *22*, 5463−5467.
(17) Dallas, P.; Tucek, J.; Jancik, D.; Kolar, M.; Panacek, A.; Zboril, R. *Adv. Funct. Mater.* **2010**, *20*, 2347−2354.
(18) Dallas, P.; Zboril, R.; Bourlinos, A. B.; Jancik, D.; Niarchos, D.; Panacek, A.; Petridis, D. *Macromol. Mater. Eng.* **2010**, *295*, 108−114.
(19) Kvitek, L.; Panacek, A.; Soukupova, J.; Kolar, M.; Vecerova, R.; Prucek, R.; Holecova, M.; Zboril, R. *J. Phys. Chem. C* **2008**, *112*, 5825−5834.
(20) Kong, H.; Jang, J. *Langmuir* **2008**, *24*, 2051−2056.
(21) Li, Z.; Lee, D.; Sheng, X.; Cohen, R. E.; Rubner, M. F. *Langmuir* **2006**, *22*, 9820−9823.
(22) Kong, H.; Jang, J. *Biomacromolecules* **2008**, *9*, 2677−2681.
(23) Kong, H.; Song, J.; Jang, J. *Macromol. Rapid Commun.* **2009**, *30*, 1350−1355.
(24) Song, J.; Song, H.; Kong, H.; Hong, J.-Y.; Jang, J. *J. Mater. Chem.* **2011**, *21*, 19317−19323.
(25) Song, J.; Kong, H.; Jang, J. *Chem. Commun.* **2009**, 5418−5420.
(26) Song, J.; Kong, H.; Jang, J. *Collid. Surface. B.* **2011**, *82*, 651−656.
(27) Tiller, J. C.; Sprich, C.; Hartmann, L. *J. Controlled Reease* **2005**, *103*, 355−367.
(28) Zasloff, M. *Nature* **2002**, *415*, 389−395.
(29) Laloyaux, X.; Fautré, E.; Blin, T.; Purohit, V.; Leprince, J.; Jouenne, T.; Jonas, A. M.; Glinel, K. *Adv. Mater.* **2010**, *22*, 5024−5028.
(30) Seyfriedsberger, G.; Rametsteiner, K.; Kern, W. *Eur. Polym. J.* **2006**, *42*, 3383−3389.
(31) Voccia, S.; Ignatova, M.; Jérôme, R.; Jérôme, C. *Langmuir* **2006**, *22*, 8607−8613.
(32) Harney, M. B.; Pant, R. R.; Fulmer, P. A.; Wynne, J. H. *ACS Appl. Mater. Interfaces* **2009**, *1*, 39−41.
(33) Bouloussa, O.; Rondelez, F.; Semetey, V. *Chem. Commun.* **2008**, 951−953.
(34) Lenoir, S.; Pagnoulle, C.; Galleni, M.; Compère, P.; Jérôme, R.; Detrembleur, C. *Biomacromolecules* **2006**, *7*, 2291−2296.
(35) Wei, Q. F.; Ye, H.; Hou, D. Y.; Wang, H. B.; Gao, W. D. *J. Appl. Polym. Sci.* **2006**, *99*, 2384−2388.
(36) Li, W. J.; Laurencin, C. T.; Caterson, E. J.; Tuan, R. S.; Ko, F. K. *J. Biomed. Mater. Res. A* **2002**, *60*, 613−621.
(37) Kong, H.; Jang, J. *Chem. Commun.* **2006**, 3010−3012.
(38) Liao, J.; Zhang, Y.; Yu, W.; Xu, L.; Ge, C.; Liu, J.; Gu, N. *Colloids Surf., A* **2003**, *223*, 177−183.
(39) Bayramgil, N. P. *J. Appl. Polym. Sci.* **2008**, *109*, 1205−1211.
(40) Huang, T.; Murray, R. W. *J. Phys. Chem. B* **2003**, *107*, 7434−7440.
(41) Cason, J. P.; Khambaswadkar, K.; Roberts, C. B. *Ind. Eng. Chem. Res.* **2000**, *39*, 4749−4755.
(42) Melaiye, A.; Simons, R. S.; Milsted, A.; Pingitore, F.; Wesdemiotis, C.; Tessier, C. A.; Youngs, W. J. *J. Med. Chem.* **2004**, *47*, 973−977.
(43) Henglein, A. *Chem. Mater.* **1998**, *10*, 444−450.
(44) Dal Lago, V.; França de Oliveira, L.; De Almeida Gonçalves, K.; Kobarg, J.; Borba Cardoso, M. *J. Mater. Chem.* **2011**, *21*, 12267−12273.
(45) Rege, K.; Raravikar, N. R.; Kim, D.-Y.; Schadler, L. S.; Ajayan, P. M.; Dordick, J. S. *Nano Lett.* **2003**, *3*, 829−832.
(46) Liong, M.; France, B.; Bradley, K. A.; Zink, J. I. *Adv. Mater.* **2009**, *21*, 1684−1689.
(47) Joerger, R.; Klaus, T.; Granqvist, C. G. *Adv. Mater.* **2000**, *12*, 407−409.
(48) Ottersbach, P.; Kossmann, B. *GIT Labor-Fachz.* **2002**, *46*, 452−456.